BIOCHEMISTRY
including biophysical chemistry & molecular biology

Article

pubs.acs.org/biochemistry

Molecular Mechanism of the Chaperone Function of Mini-α-Crystallin, a 19-Residue Peptide of Human α-Crystallin

Priya R. Banerjee,[†] Ajay Pande, Alexander Shekhtman, and Jayanti Pande*

Department of Chemistry, Life Sciences, University at Albany, State University of New York, Albany, New York 12222, United States

Supporting Information

ABSTRACT: α-Crystallin is the archetypical chaperone of the small heat-shock protein family, all members of which contain the so-called "α-crystallin domain" (ACD). This domain and the N- and C-terminal extensions are considered the main functional units in its chaperone function. Previous studies have shown that a 19-residue fragment of the ACD of human αA-crystallin called mini-αA-crystallin (MAC) shows chaperone properties similar to those of the parent protein. Subsequent studies have confirmed the function of this peptide, but no studies have addressed the mechanistic basis for the chaperone function of MAC. Using human γD-crystallin (HGD), a key substrate protein for parent α-crystallin in the ocular lens, we show here that MAC not only protects HGD from aggregation during thermal and chemical unfolding but also binds weakly and reversibly to HGD ($K_d \approx$ 200−700 μM) even when HGD is in the native state. However, at temperatures favoring the unfolding of HGD, MAC forms a stable complex with HGD similar to parent α-crystallin. Using nuclear magnetic resonance spectroscopy, we identify the residues in HGD that are involved in these two modes of binding and show that MAC protects HGD from aggregation by binding to Phe 56 and Val 132 at the domain interface of the target protein, and residues Val 164 to Leu 167 in the core of the C-terminal domain. Furthermore, we suggest that the low-affinity, reversible binding of MAC on the surface of HGD in the native state is involved in facilitating its binding to both the domain interface and core regions during the early stages of the unfolding of HGD. This work highlights some structural features of MAC and MAC-like peptides that affect their chaperone activity and can potentially be manipulated for translational studies.

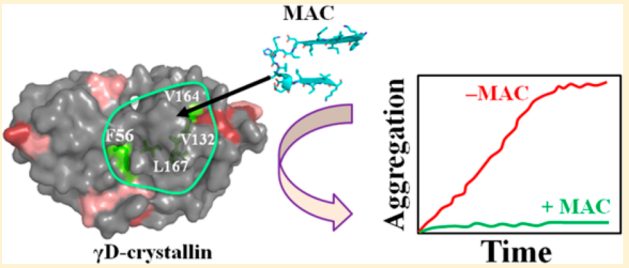

An important function of the small heat-shock proteins (sHSPs) is to prevent target (also called substrate or client) proteins from aggregating under conditions that promote protein unfolding. Although sHSPs are present in all kingdoms of life,[1] the best characterized members of the family are the α-crystallins, found in the ocular lens. Because the protein concentration in the lens fiber cells is unusually high, and protein turnover is negligible,[2] it is easy to appreciate the role of these proteins in preventing aggregation and, hence, light scattering *in vivo*. It is now generally accepted that sHSPs are among the first responders of the cell to various stress signals[3] and that they are rather promiscuous and non-discriminating in the selection of their substrates[4]—yet the chaperone function of the α-crystallins, or sHSPs in general, is not as well understood at the molecular level[5] as that of the ATP-dependent chaperone systems.[6] Moreover, the structure of the bound target protein is not known and still remains an active area of research.[7]

The chaperone activity of the α-crystallins is experimentally measured *in vitro* using target substrates under conditions that induce protein unfolding and aggregation, such as heating, disulfide reduction, or by means of known chemical denaturants.[8−11] Several structural features in the α-crystallins and other sHSPs are believed to be responsible for their chaperone activity. Prominent among them is the common domain in all sHSPs, the so-called α-crystallin domain (ACD), comprising the core β-sheet structure consisting of nine β-strands (B1−B9).[12] Oligomerization of the α-crystallins or even dimerization leads to interfacial grooves and surrounding pockets that have been proposed as the hydrophobic substrate binding sites.[1,12] The mostly disordered N-terminal stretch (∼55 residues) flanking the ACD has also been implicated in substrate binding and is believed to undergo conformational changes adapting to any substrate, which explains the versatility of sHSPs in binding a variety of substrates.[13] Finally, the C-terminal tail of ∼20 residues has been implicated in the recognition and selection of substrate proteins.[14,15] It also contains the IXI/V motif, thought to be important for oligomerization[16] which in turn is important for substrate binding.

In view of these functionally significant complex structural features, it is surprising that a 19-residue peptide fragment from the ACD of human αA-crystallin, called mini-αA-crystallin (or MAC),[17−19] which has almost none of these structural features and consists of only parts of β-strands B3 and B4 of ACD, still shows chaperone activity similar to that of the parent protein toward the substrates examined so far. Historically, this peptide was first synthesized by Sharma et al.,[18] on the basis of their

Received: November 22, 2014
Published: December 5, 2014

DOI: 10.1021/bi5014479
Biochemistry 2015, 54, 505−515

findings that it contained the binding site for mellitin and bis-ANS in α-crystallin, and the binding diminished the chaperone activity of the crystallin. This intriguing chaperone property of the peptide prompted us to undertake our investigation. In exciting new developments, several reports have indicated that MAC-related peptides also show inhibitory effects on apoptosis similar to that of the α-crystallins.[20,21] In addition, Steinman and co-workers[22,23] have shown such peptides to have a therapeutic effect in multiple sclerosis and neuro-inflammation, as well. Thus, peptides such as MAC are interesting not only as peptide chaperones but also independently as therapeutic agents that can potentially be developed for translational studies.[24]

These novel advances prompted us to undertake a detailed investigation of MAC, and in the work reported here, we characterize its solution structure and probe its chaperone activity toward a lens-specific substrate protein, human γD-crystallin (HGD), which is a natural substrate for parent α-crystallin.[25] We found that MAC not only exhibits chaperone-like activity toward HGD in our assays but also forms a stable complex with HGD. Our data show that while ∼30% of HGD is present in an irreversible complex with the peptide, there are only minor changes in the structure of HGD in the MAC-bound state.

MATERIALS AND METHODS

Cloning, Expression, and Purification of the Target Protein and Peptide. Cloning, expression, and purification of HGD[26] as well as the preparation of [U-^{15}N]HGD were conducted as described previously.[27] Extraction and purification of bovine α-crystallin were performed as reported previously.[28] Unlabeled MAC (DFVIFLDVKHFSPEDLTVK) was purchased from GenScript, and because it was ∼96% pure, no further purification was conducted. The [^{15}N]Val-labeled MAC was ∼95% pure and synthesized by LifeTein, LLC. The peptide samples were subjected to extensive dialysis against water and lyophilized for 48 h to remove any traces of residual trifluoroacetic acid (TFA) remaining from previous purification steps during synthesis.

With the exception of peptide solutions used in the CD studies, all solutions of MAC were made by weighing the lyophilized peptide. Concentrations of the MAC solutions used in CD studies were determined more accurately as described below.

CD Spectroscopy. Two methods were adopted to measure the concentrations of MAC solutions used for the CD studies shown in Figure 1A: (1) gravimetric method and (2) UV absorption. The gravimetric method involved the following procedure. The MAC preparation purchased from GenScript was extensively dialyzed against doubly distilled water and lyophilized. A stock solution was prepared in doubly distilled water from the lyophilized material, from which a known volume (100 μL aliquot) was taken in a preweighed aluminum pan. The pan was heated to 125 °C in an oven for 2 h, cooled in a desiccator, and weighed. The cycle was repeated until a constant weight was obtained. The second method involved measuring the UV absorption spectrum of the stock solution after dilution in 100 mM sodium phosphate buffer (pH 7) containing 4 M guanidinium hydrochloride (GdnHCl). The concentration of MAC was calculated using a molar extinction coefficient of 195 at 258 nm for each of the three Phe residues[29] in MAC. The concentration thus determined was ∼10% lower than that determined gravimetrically. We did not use the gravimetric data in the event that residual salts were still present in the peptide solution and led to the higher concentration estimate. Thus, the concentration of MAC used here is based solely on the absorption data shown in Figure 1B, which are essentially caused by the UV absorption of Phe.

CD spectra were recorded on a JASCO J-815 spectropolarimeter equipped with a Peltier type temperature controller. The protein concentration was 0.1 mg/mL for CD spectral measurements in the far-UV range in low-ionic strength (5 mM) phosphate buffer (pH 7). We used a low-ionic strength buffer in this region because it allowed us to measure the CD signal down to 190 nm with low noise.

Chaperone Assays. Two methods were used to assay the chaperone activity of MAC. In the first method, the published procedure of Acosta-Simpson[30] was followed and is described here briefly. Aggregation of HGD was triggered by a rapid dilution of the denaturant, GdnHCl, from 6 to 0.5 M during the refolding of unfolded protein in 100 mM sodium phosphate buffer (pH 7) at 25 °C (Figure 2A). The mixing dead time in these experiments was 60 s.

In the second method, the turbidity of HGD solutions was measured at 68 °C in 100 mM sodium phosphate buffer (pH 7) as a function of time by recording the absorbance at 350 nm in a Cary 100 UV−vis spectrophotometer equipped with an automated temperature controller (Figure 2B). Protein and peptide concentrations and their molar ratios used in both assays are mentioned in the appropriate sections in the text and figures.

NMR Spectroscopy. NMR data were acquired on a Bruker Avance III 500 MHz spectrometer equipped with an ultrasensitive TCI triple-resonance cryo-probe, and a Bruker Avance II 400 MHz spectrometer equipped with a standard TBI probe. Both NMR spectrometers are capable of applying pulsed field gradients along the *z*-axis.

NMR samples were prepared by dissolving variable concentrations of proteins in NMR buffer [10 mM potassium phosphate (pH 7)].[27] MAC solutions of increasing concentrations, in the same buffer as the target protein, were used to titrate the target protein solution maintained at a fixed concentration (50 μM). To make the irreversible complex, labeled (or unlabeled) MAC was used at a concentration 8−10-fold higher than that of HGD and incubated at a temperature around 60 °C for 10−12 h. A ^{15}N-edited HSQC, ^{1}H−^{15}N HSQC, NMR experiment was used to monitor complex formation.[31] Water suppression during NMR experiments was achieved by using the WATERGATE pulse sequence.[32] All experiments were conducted at 25 °C unless otherwise noted. Variable-temperature NMR measurements were taken on a Bruker 400 MHz spectrometer with a protein concentration of 100 μM, in the presence and absence of 300 μM MAC in NMR buffer. All data were analyzed using the NMR program CARA.[33] Chemical shift perturbations (CSPs) were calculated as described previously.[27] Binding isotherms were analyzed and K_d values estimated with the following equation using OriginPro 8:

$$\Delta\delta = \frac{\Delta\delta^{max}\cdot[L]}{K_d + [L]};\ \Delta\delta = \text{CSP};\ L = \text{ligand (MAC)} \quad (1)$$

Structural Modeling. Surface maps were generated using PyMol (DeLano Scientific). Molecular models of MAC were generated using DS ViewerPro (Accelrys).

DOI: 10.1021/bi5014479
Biochemistry 2015, 54, 505−515

RESULTS

Our results consist of the following key elements: (i) characterization of the general spectral properties of MAC and its thermal stability, (ii) demonstration of the chaperone-like properties of MAC with HGD as the target protein using two different assays, (iii) NMR studies of the binding of MAC to [U-^{15}N]HGD at various temperatures at which both HGD and MAC are in the native, folded state (these experiments show that MAC binds weakly and reversibly to HGD under ambient conditions), (iv) NMR studies of the binding of MAC to [U-^{15}N]HGD at high temperatures (NMR measurements were taken at high temperatures with HGD alone and in a mixture with MAC at several temperatures, including those at which the thermal unfolding of HGD was initiated; these measurements were designed to detect the residues of HGD affected by MAC binding at the initial stages of structural perturbation as HGD underwent thermal destabilization), (v) NMR studies of MAC bound irreversibly to [U-^{15}N]HGD (i.e., the chaperone−substrate complex), and (vi) NMR studies of MAC (labeled with [^{15}N]valine) bound to unlabeled HGD in the chaperone−substrate complex. Thus, data from sections (i) and (ii) describe the properties of MAC and demonstrate its chaperone activity in different assays. Data from section (iii) show that MAC binds weakly to HGD even when HGD is in the native conformation. These data provide a structural and thermodynamic understanding of such a binding process. We find that this type of binding is reversible upon dialysis, unlike the binding at higher temperatures (as in section (iv), closer to the unfolding temperature of HGD). This second type of binding results in a MAC−HGD complex that is stable upon exhaustive dialysis. In sections (v) and (vi), we investigate the MAC−HGD complex formed in section (iv).

(i) Structure and Stability of MAC. The peptide sequence of MAC used in the studies reported here is ^{70}DFVIFLDVK-HFSPEDLTVK^{88}, which is identical to that of the actual peptide fragment from human αA-crystallin, except at position 70, which is a lysine in the parent protein. We replaced Lys 70 with Asp on the basis of the work of Sharma and co-workers,[34] who were the first to use both forms of the peptide interchangeably naming them mini-αA-crystallin. They also showed that both MAC peptides are effective chaperones,[18] and in most of their work,[17,34−37] including their recent paper,[38] they have used the Asp 70 peptide. We also note that several similar peptides with chaperone activity have been used by other investigators in their studies,[20,39] particularly the MAC peptide with an acetylated Lys 70 used by Nahomi et al.[20] that shows a chaperone activity *in vitro* ∼15% higher than that of the nonacetylated peptide for the γ-crystallin substrate. It should be mentioned, however, that MAC or MAC-like peptides have not been found in the ocular lens *in vivo*, and the purpose of our work is merely to identify the structural basis of the chaperone function of the MAC-like peptides *in vitro*.

Figure 1A shows the CD spectra of MAC solutions subjected to serial dilution in 5 mM sodium phosphate buffer (pH 7). The corresponding absorption spectra, which scale linearly with each successive dilution, are shown in Figure 1B. However, as is apparent from the CD spectra, at 455 μM [the highest concentration used (Figure 1A, black curve)], MAC is predominantly present in the β-sheet form with a typical CD minimum around ∼218 nm. Upon dilution to concentrations below 225 μM, MAC showed an increasing population of the disordered form, as observed by the gradual shift of the CD

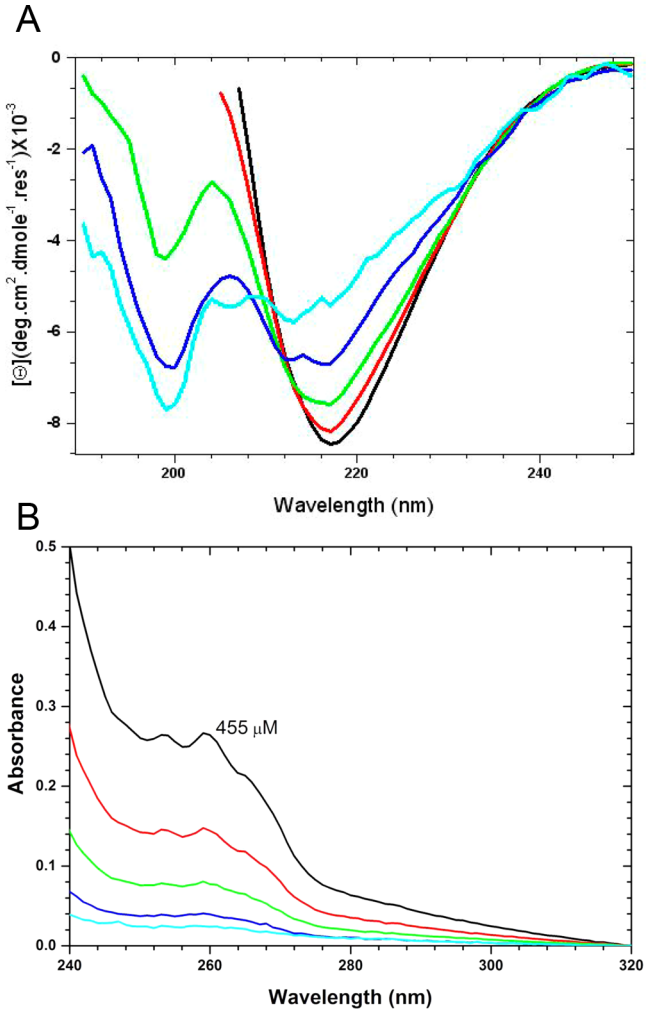

Figure 1. (A) CD spectra of MAC (mini-αA-crystallin) in 5 mM phosphate buffer (pH 7) showing the effect of serial dilution as the concentration is lowered from 455 to 28 μM. Each spectrum is an average of nine scans. Spectra at the two highest concentrations were truncated at 204 nm because of detector saturation. Dilution leads to a shift in the CD minimum from ∼218 to ∼200 nm, indicating a conformational transition from a β-sheet structure to a random coil. The spectra (all except the one corresponding to the lowest protein concentration) show an isodichroic point at 212 nm, indicating the equilibrium between the two conformations of the peptide. (B) Absorption spectra of MAC in 5 mM phosphate buffer (pH 7). Spectra measured at concentrations ranging from 455 to 28 μM obtained by serial dilutions appear to scale linearly. The main phenylalanine band at 257 nm is clearly visible and has been used for the concentration measurements in (A). In addition, the phenylalanine bands at 252 and 263 nm are also observed, but not that at 246 nm. Because MAC does not contain any other aromatic residues besides phenylalanine, the UV absorbance at 257 nm is likely to be solely caused by phenylalanine.

minimum to a final value approaching 200 nm. Thus, the secondary structure of MAC is transformed from a predominantly β-strand form at concentrations of ≥225 μM to one that is almost entirely disordered at a 10-fold lower concentration. This type of concentration-dependent conformational transition has also been observed for other peptides, especially those forming β-hairpins or β-sheets.[40,41] Thus, the peculiar behavior of MAC suggests that it may be present in solution as reversible oligomers and that such oligomerization above a

DOI: 10.1021/bi5014479
Biochemistry 2015, 54, 505−515

threshold peptide concentration probably promotes the formation of the β-sheet structure. We observed a similar equilibrium also in high-ionic strength buffers, but the higher ionic strength [100 mM sodium phosphate (pH 7)] shifts the equilibrium toward the β-sheet form (data not shown). The data shown here reveal this equilibrium clearly, because of the negligible optical interference (and hence better signal to noise ratio) in the far-UV region using the low-ionic strength (5 mM sodium phosphate) buffer.

Previous studies[17] have reported that MAC assumes a β-sheet-rich secondary structure that is retained until 55 °C and is necessary for its chaperone property. Although our peptide has a similar fold (Figure 1A), we observe a much higher unfolding temperature with a transition midpoint around 85 °C (Figures S1A and S1B). This holds for all the peptide preparations used in this work. Figure S1B shows that the structural transition could not be followed to completion because of the high temperatures required for unfolding, which is evident in the sigmoidal fit to the transition. For this reason, we have not attempted to analyze the data rigorously and simply suggested an approximate midpoint for the unfolding transition of MAC. It is noteworthy that MAC has a high melting temperature and is thus able to function as a chaperone at significantly high temperatures, such as 68 °C, which is used in this study (see below).

To better understand the interaction of MAC with HGD, we modeled the three-dimensional structure of MAC using the PEP-FOLD server,[42,43] which uses a *de novo* approach to model the structures of small peptides based on the consecutive sequences of four-residue structural units. Three representative models are shown in Figure S2A. All the models show a hairpin structure with a hairpin length around 20−25 Å, while some show canonical turns. We find that the MAC segment within the parent protein, αA-crystallin, does not form a β-hairpin but, instead, contains parts of two different β-strands (Figure S2B). Thus, there was no *a priori* knowledge that MAC would necessarily fold into a β-sheet structure. Furthermore, to examine the propensity of MAC for a particular secondary structure, we used the PSIPRED server (http://bioinf.cs.ucl.ac.uk/psipred; Figure S2C). The prediction shows that six residues in the N-terminal end and two in the C-terminal end form a β-strand while all others are ambivalent and in the "coil" form. It is likely that these β-strands nucleate the formation of the hairpin structure of the peptide in solution. Therefore, higher concentrations seem to favor the β-sheet structure in the peptide.

(ii) Chaperone Activity of MAC toward HGD. MAC has been shown to prevent the aggregation of several proteins *in vitro*,[17,35,36] including the γ-crystallins[20,37] which are important because they are natural substrates of α-crystallin. Notably, Kumar et al.[37] have shown that MAC is effective in protecting the γ-crystallins from oxidative insults. However, to conduct a detailed mechanistic study of the protection process, we chose human γD-crystallin, which is a homogeneous single protein, rather than a family of γ-crystallins. To test the chaperone function of MAC with HGD, we used two different aggregation conditions: (a) as in ref 30, using a concentration jump from high denaturant to low denaturant concentration (from 6 to 0.5 M GdnHCl) and monitoring the resulting scattering over a period of time (Figure 2A), and (b) heating HGD to 68 °C and monitoring the scattering for a similar time period (Figure 2B). In both cases, HGD alone, in the absence of MAC, formed visible aggregates which resulted in increased turbidity in

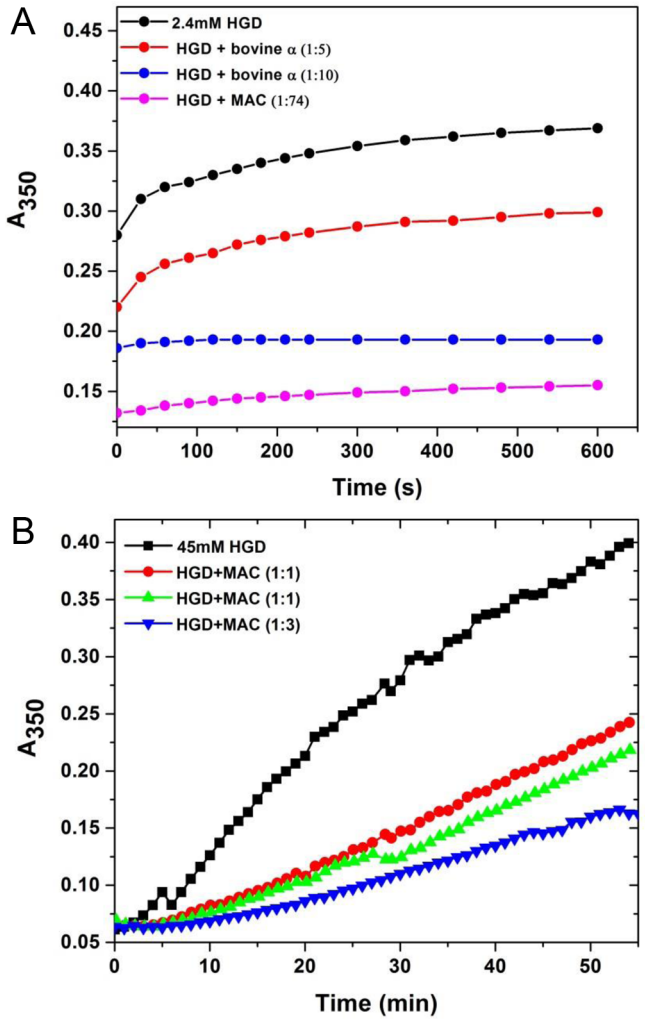

Figure 2. (A) Chaperone activity of MAC toward HGD. In assay 1, aggregation of HGD was initiated by rapid dilution of GdnHCl from 6 to 0.5 M and monitored by measuring the turbidity at 350 nm. The final HGD concentration was 0.05 mg/mL (2.4 μM), in the presence (blue) and absence (black) of 178 μM MAC. For control measurements, bovine α-crystallin wad used (red and green). The assay clearly shows the anti-aggregation property of MAC. The points are experimental data. Lines are guides to the eye. (B) Chaperone activity of MAC toward HGD. In assay 2, aggregation of HGD was initiated by incubating the protein at 68 °C in the absence and presence of various amounts of MAC (mole:mole) as indicated. The data suggest that the peptide is capable of efficiently suppressing thermally induced aggregation of HGD in a dose-dependent manner. The points are experimental data. Lines are guides to the eye.

solution as measured by light scattering at 350 nm (A_{350}). However, as shown in panels A and B of Figure 2 in the presence of MAC, the aggregation of HGD was effectively suppressed in both assays. In the first assay (a), the concentrations of HGD (0.05 mg/mL or 2.4 μM) and bovine α-crystallin as a control (0.25 mg/mL) were consistent with those of Acosta-Sampson.[30] An 8-fold higher (w/w) concentration of MAC (177.8 μM, 74-fold molar excess) compared to that of HGD showed dramatic suppression of aggregation (Figure 2A). In the second assay (b), a higher concentration (1.0 mg/mL or 48.5 μM) of HGD was used and a 1:1 molar concentration of MAC was found to be effective. Furthermore, in this assay, we attempted to observe the "dose response" by

DOI: 10.1021/bi5014479
Biochemistry 2015, 54, 505−515

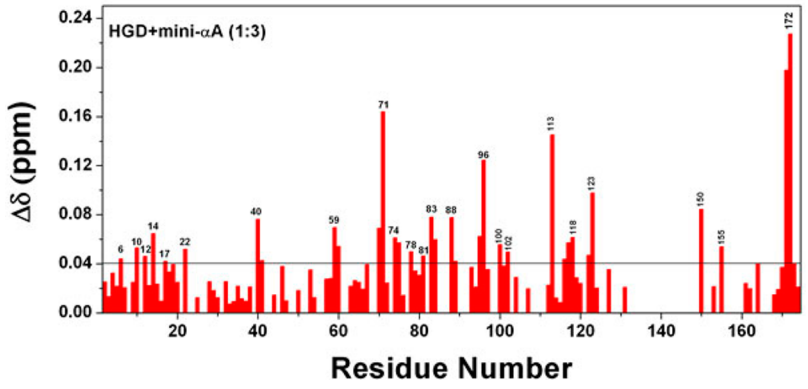

Figure 3. HSQC spectrum of HGD (50 μM) showing the amide chemical shift perturbations caused by interactions with MAC. Shown here are average shifts for all assigned residues in HGD[27] as a result of interaction with MAC (1:3 HGD:peptide molar ratio). The mixture was heated at 68 °C for 40 min and then cooled to 25 °C before the spectrum was recorded. The HSQC spectrum of this "heated mixture" is identical to that of the mixture at room temperature that was never heated.

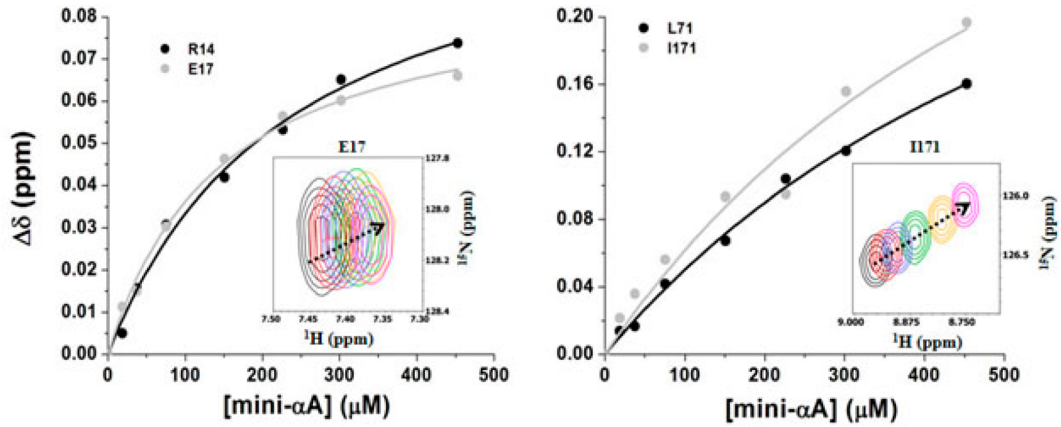

Figure 4. Multiple binding sites of MAC on HGD. NMR titration of HGD (50 μM) with increasing concentrations of MAC showing representative binding isotherms with a binding affinity of <350 μM (left) and representative binding isotherms with a binding affinity of >400 μM (right). The insets show progressive chemical shift perturbation of Glu 17 and Ile 171 (left and right, respectively), with increasing peptide concentrations (indicated by an arrow). All residues of HGD that interact with the peptide under these conditions (see Figure 6A and Table S1), can be described by either of these binding isotherms.

increasing the HGD:MAC ratio from 1:1 to 1:2 and 1:3 (mole:mole) and found that increasing concentrations of MAC were correspondingly more effective in suppressing the aggregation of HGD (Figure 2B).

(iii) Structural Characterization of HGD−MAC Interactions. We used high-resolution solution NMR spectroscopy to probe the interactions between HGD and MAC. We first recorded the ^{1}H−^{15}N HSQC spectrum of HGD in the presence of the peptide at 25 °C after they were preheated together at 68 °C for 40 min, conditions similar to those used for the *in vitro* chaperone assays described above. On the basis of our earlier backbone assignment of HGD,[27] we observed moderate chemical shift perturbations (CSPs) for a number of residues in HGD (Figure 3), in both the N- and C-terminal domains, suggesting regions on the substrate (or target) protein that are involved in interacting with the peptide. Interestingly, however, we observed identical shifts in the ^{1}H−^{15}N HSQC spectrum of [U-^{15}N]HGD in the presence of MAC, even when the step of preheating to 68 °C was eliminated. In addition, we also noticed that extensive dialysis of both mixtures (preheated and unheated) with a 10 kDa molecular mass cutoff membrane removed all of the MAC peptide and restored the original ^{1}H−^{15}N HSQC spectrum of [U-^{15}N]HGD in each case. These results suggest that while heating to 68 °C for 1 h is sufficient to generate adequate amounts of unfolded, aggregated HGD that can be observed by optical scattering, not enough of a stable form of the HGD−MAC complex that can be tracked by NMR is generated under these conditions. More importantly, it was apparent from these data that simply mixing HGD and MAC even at ambient temperatures produced shifts in the ^{1}H−^{15}N HSQC spectrum of [U-^{15}N]HGD arising from the binding of MAC to native, folded HGD.

To better define this type of weak or reversible binding (we have used these terms interchangeably in the following sections), we titrated [U-^{15}N]HGD with MAC at 25 °C (i.e., without preheating) and measured the ^{1}H−^{15}N HSQC spectra as a function of increasing concentrations of MAC. The corresponding binding isotherms are shown in Figure 4, which reveals two sets of residues: one with an apparent K_d of ∼200 μM (Figure 4, left panel) and the other with an apparent K_d of ∼700 μM (Figure 4, right panel). In the inset to each figure, the progressive chemical shift changes of a representative residue are shown. These affinity values are consistent with a weak binding interaction between HGD and MAC, under these conditions. For the titrations shown in the right panel (i.e., K_d ≅ 700 μM), the K_d value was calculated using only the initial

DOI: 10.1021/bi5014479
Biochemistry 2015, 54, 505−515

part of the titration because the low solubility of MAC limited the measurements at higher concentrations. Therefore, the K_d values in these cases are likely to be less accurate than those shown in the left panel and should be viewed as lower estimates of the actual K_d values. Both K_d values have been calculated assuming a standard single-site binding model (see Materials and Methods). We found that all residues of HGD that interact with MAC can be described by either one of these binding isotherms (see also Figure 6A and Table S1). Interestingly, among these are two residues, Tyr 6 and Ser 123, that also participate in irreversible binding with MAC, which is discussed below.

(iv) NMR Studies of the Binding of MAC to [U-^{15}N]HGD at High Temperatures. To ascertain whether HGD binds to MAC in a different manner at higher temperatures that favor thermal unfolding (as compared with the binding at ambient temperature discussed in section (iii)), we performed a ^{1}H−^{15}N HSQC measurement of [U-^{15}N]HGD in the presence and absence of MAC as the protein solution was heated to temperatures ranging from 25 to 65 °C at intervals of 2−5 °C. Selecting a range of temperatures was important for the following reason. Temperature has a pronounced effect on the chemical shift of each amino acid residue, and a gradual, linear, and unidirectional shift of each cross-peak is typically expected as the temperature is increased.[44] Therefore, any deviation from linearity and/or the appearance of new cross-peaks would indicate new interaction sites for MAC on HGD at the higher temperatures. Despite several differences in the two spectra, one with HGD alone and the other with HGD and MAC (Figure 5), the only

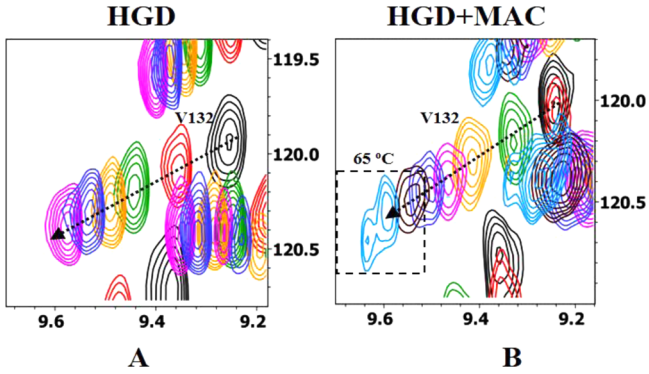

Figure 5. Interaction of Val 132 of HGD with MAC at 65 °C, (B) showing the appearance of a new peak in the HSQC spectrum of HGD [25 (red), 35 (green), 45 (orange), 50 (pink), 55 (blue), 60 (wine), and 65 °C (cyan)]. The corresponding reference HSQC spectra for HGD are shown in panel A [25 (black), 35 (red), 45 (green), 50 (orange), 55 (blue), and 60 °C (pink)]. The arrows indicate the direction of the temperature increase.

cross-peak that could be assigned unambiguously in the mixture was that arising from Val 132 at 65 °C. This suggests that this particular residue interacts with the minichaperone at 65 °C as the substrate protein (HGD) begins to unfold.

(v) NMR Study of the Irreversible Complex of [U-^{15}N]HGD and MAC. To increase the yield of the irreversible HGD−MAC complex, we incubated a mixture of HGD and MAC at 60 °C for an extended period of time (~24 h). In an earlier study, we had shown that as much as 20% of HGD binds to human αA-crystallin upon being incubated at 55 °C for 16 h.[45] In the study presented here, we observed that HGD alone almost completely precipitates from solution upon incubation at 60 °C for 24 h, while only a small fraction precipitates if the solution is heated in the presence of MAC. After being heated, the supernatant was extensively dialyzed with a 10 kDa molecular mass cutoff membrane to remove the unbound and weakly bound MAC before the ^{1}H−^{15}N HSQC spectra of [U-^{15}N]HGD irreversibly bound to MAC were recorded.

We found three types of changes. Several residues gave rise to new peaks; peak broadening was observed in some cases (Figure 6B), and minor chemical shift perturbation (CSP) was also observed for some residues (Figure S3 and Table S2). Residues that showed new peaks are Tyr 6, Asp 38, Gln 54, Phe 56, Asp 61, Asp 97, Glu 107, Ser 123, Ser 130, Val 132, Arg 152, Ser 166, Leu 167, and Ser 174. In addition, Asn 138, Val 164, and Gly 165 showed significant line broadening. This new set of residues showing spectral changes due to the irreversible binding of the peptide to HGD is different from the set of residues that show CSP at ambient temperatures (see section (iii), Figure 3), except for Tyr 6 and Ser 123, which are common to both. These residues are mapped on the crystal structure of HGD[46] (Figure 7). We have also computed the relative population of the MAC−HGD complex by comparing the intensities of the original cross-peaks in the spectrum of free HGD with those of the newly observed cross-peaks of Phe 56, Val 132, Ser 166, and Leu 167 in the spectrum of the complex. These comparisons show that 31.8 ± 5.8% of HGD is present in the form of the HGD−MAC complex.

Besides the residues giving rise to new peaks, and showing line broadening, we also observe minor CSPs for a small set of residues (Figure S3 and Table S2). These are listed primarily for the sake of completeness. In Figure S3, we have taken 0.015 as an arbitrary cutoff to denote significant CSPs. As noted in Table S2, there are two residues (V75 and E96) of HGD that are also observed to bind reversibly to MAC. However, because the absolute values of CSPs is this case are quite small, these residues are not our primary interest, and we will first focus on residues that show new cross-peaks and line broadening and return to these residues later in this section.

(vi) Binding of [^{15}N]Val-Labeled MAC to HGD. To confirm that MAC is in fact irreversibly bound to HGD, [^{15}N]Val-labeled MAC was used to conduct an experiment similar to that described in section (v), and the ^{1}H−^{15}N HSQC spectrum of the HGD−[^{15}N]Val-MAC complex was recorded. When compared with the reference spectrum of the free [^{15}N]Val-labeled MAC at room temperature, we observed severe line broadening of all the cross-peaks in the complex (Figure 8). We observed four cross-peaks from free [^{15}N]Val-labeled MAC, even though there are only three Val residues in the peptide, which is somewhat surprising. This is most likely a reflection of the structural heterogeneity in the peptide caused by its concentration-dependent oligomerization already shown and discussed in Figure 1. While this experiment was performed mainly to determine the extent of the binding of MAC to HGD, we were unable to derive such information because of the severe line broadening of all cross-peaks pertaining to the ^{15}N-labeled valines in the peptide.

From the list of residues in HGD, which participate in "irreversible" binding to MAC (Table S3), we selected those that are not solvent-accessible (highlighted in Table S3) in the native protein. These residues were selected as follows. First, the solvent accessibilities of all residues of HGD (Protein Data Bank entry 1hk0) were computed as relative exposed fractional

DOI: 10.1021/bi5014479
Biochemistry 2015, 54, 505−515

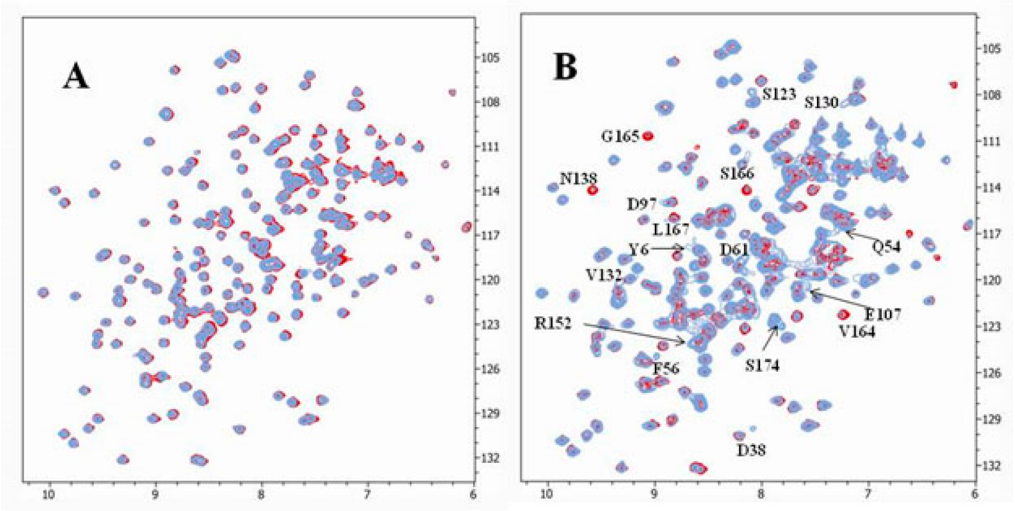

Figure 6. Overlay of the HSQC spectra of HGD (red contours) and HGD with MAC (blue contours) measured at 25 °C. (A) Reversible binding. The HGD/MAC mixture was heated for 1 h, followed by extensive dialysis. As described in the text, HSQC spectra are identical with or without heating. (B) Irreversible binding. The HGD/MAC mixture was heated for 24 h at 60 °C followed by extensive dialysis (see the text for details). The residues of HGD that interact with the peptide (new peaks and/or broadening) are marked.

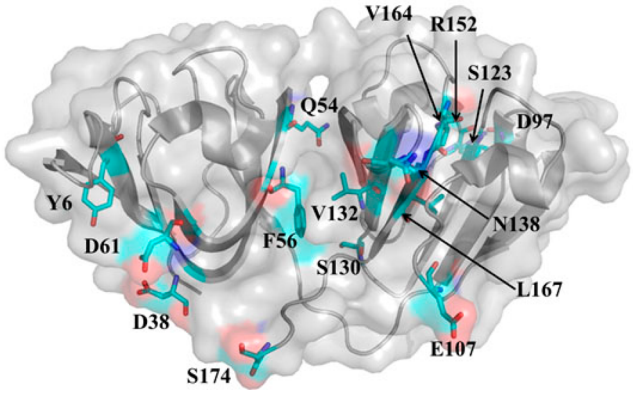

Figure 7. Crystal structure of HGD (Protein Data Bank entry 1HK0) showing a map of the residues (from Figure 6B) that are perturbed in the binding of MAC in the irreversible complex.

surface areas using ASA-View, a Web server (www.abren.net/asaview/). Then, using an arbitrary cutoff value of 0.1, these residues were divided into two classes: solvent-accessible and solvent-inaccessible. A cursory look at the solvent-accessible residues indicates that they are all charged and/or polar. Notable among them is Asp 97, which is known to be involved in a charge network cluster propagated with water molecules.[46] Thus, it is likely that the effect we observe in the surface residues (i.e., the nonhighlighted residues in Table S3) is related to the perturbation in the surface charge network along with the adjoining water layer. It is also evident that all these residues are among those that generally make most of the water-mediated contacts in proteins.[47]

The group of solvent-inaccessible residues in Table S3 consists mainly of hydrophobic amino acids and three serine residues. Of these, Ser 130 (Table S4) is capable of forming hydrogen bonds with water directly and is also involved in the reversible binding with MAC. Thus, it appears sufficiently surface-exposed to interact with the hydration layer. Ser 123, on the other hand, appears to be H-bonded to two other residues (Tyr 93 and 98) that interact with the hydration layer extensively (Table S5). Furthermore, a careful examination of the structure of HGD shows that Ser 123 may be in a deep crevice, and water molecules in such crevices are often missed in crystallographic studies.[48] Therefore, we consider these two Ser residues, 123 and 130, as solvent-accessible and not directly affected by MAC binding. That leaves six residues, namely, Phe 56, Val 132, and Ser 164−Leu 167, that define the binding locus for MAC. Among these, Phe 56 and Val 132 are in the domain interface, belonging to a β-strand in the N- and C-terminal domains, respectively (Figure 7). The four remaining residues (164−167) are contiguous and in the last (C-terminal) edge strand. Thus, we suggest that residues 56, 132, and 164−167 define the binding locus of MAC to the normally solvent-inaccessible, or partially accessible surface of HGD, thereby protecting it from solvent exposure and consequent aggregation.

The edge strand containing residues 164−167 interacts with the adjacent strand containing residues 130−135 and is protected[49] from intermolecular interactions by two loops, one containing residues 106−118 and another containing residues 136−141. We note (Figure S3 and Table S2) that E135 of the adjacent strand and C109 of one loop show minor CSPs. This is consistent with our identification of the putative MAC binding locus. Furthermore, L112 (of the former loop) may also have a new cross-peak, but its identification is ambiguous, as L112 and I81 have overlapping cross-peaks in native HGD (data not shown). From the residues listed in Table S2, we have thus identified those that are also involved in reversible (transient) binding to the native protein, as well as those that we believe are directly perturbed by the binding of MAC to the putative locus in heat-destabilized HGD. Note that the two remaining residues in Table S2, M102 and I103, are both solvent-accessible. Because we are mainly interested in those residues that are surface-inaccessible, as they are the ones most likely to be involved in unfolding and protected by MAC binding, we have not considered these two surface residues further.

In identifying residues that show CSPs in the $^{1}H-^{15}N$ HSQC NMR spectra, one must be cautious about "false positives" for CSP,[50] which may arise if the binding leads to local structural changes in the protein backbone (as indicated above in section

DOI: 10.1021/bi5014479
Biochemistry 2015, 54, 505−515

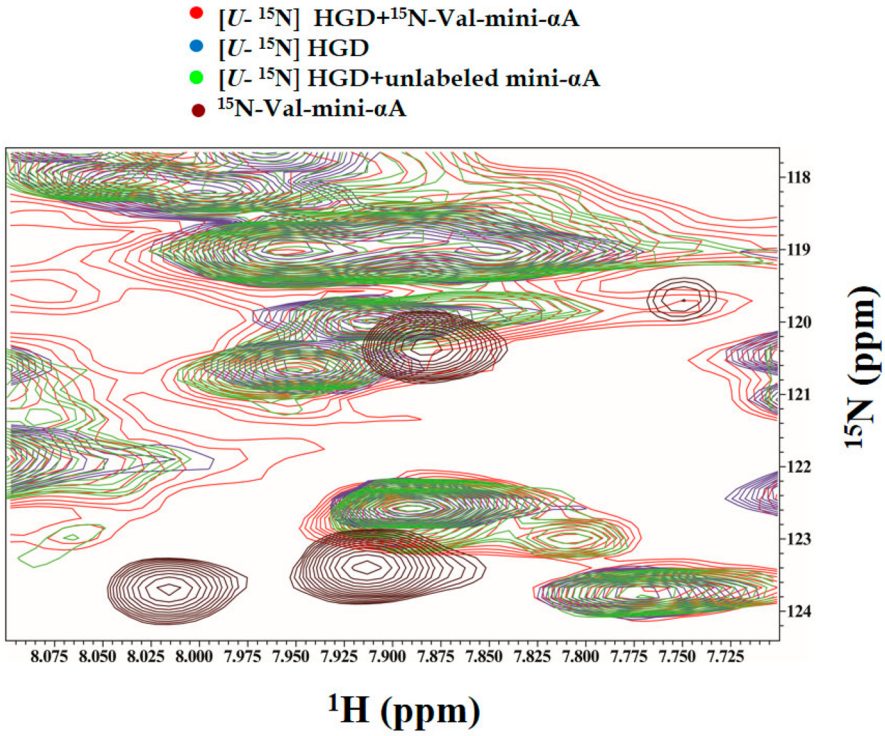

Figure 8. Limited region of the HSQC spectra of the HGD−MAC irreversible complex. The color code for each spectrum is shown. [^{15}N]Val peaks in MAC alone and MAC in the molecular complex with HGD are observed.

(iii)). However, despite this caveat, determination of CSPs plays an important role in characterizing binding of ligand to proteins.[50,51] Here we have tried to make the case that except for these six (of the total of 17 residues in Table S3), other residues may show CSPs not directly caused by the binding of MAC but by local structural perturbations and adjustments as a result of perturbation in the charge network and the associated hydration layer. Clearly, we do not have evidence of the proposed role for the charge network and hydration layer, and the changes we observe may be due to direct binding of MAC to these residues, as well, or a combination of the two effects. However, our proposal is plausible, because binding of ligand to proteins requires a serious consideration of the water network, as has been shown recently by Breiten et al.[52] It should also be noted that our analysis involving the hydration layer is made possible by the availability of the high-resolution crystal structure of HGD,[46] which clearly shows the locations of the water molecules in the hydration shell.

DISCUSSION

Our data show that MAC is effective as a molecular chaperone for HGD, a natural substrate for the parent protein, α-crystallin. Although Nahomi et al.[20] and Kumar et al.[37] have already shown MAC to be effective in protecting γ-crystallins from aggregation and oxidation, respectively, it has never before been tested in the unfolding process of HGD. Furthermore, our observation that MAC exhibits β-sheet structure that remains stable to very high temperatures in solution ($T_m \sim 85$ °C) is a new finding. We also found that the β-sheet structure of MAC is related to its aggregation state because MAC is gradually converted to a disordered structure upon dilution and at low salt concentrations. It is conceivable that such an equilibrium results in a rudimentary pool of heterogeneous oligomeric conformations similar to that observed in parent α-crystallin.[53] In α-crystallin and other small heat-shock proteins, such structural heterogeneity and the associated dynamic exchange of subunits are believed to be responsible for the versatility in their chaperone function toward a diverse array of targets.

An important finding in this work is that MAC binds to HGD at ambient temperatures where HGD is in its native, folded form, as well as at substantially high temperatures at which HGD normally unfolds. At ambient temperatures, it binds weakly and reversibly with apparent K_d values in the range of 200−700 μM. This binding is reversible upon dialysis, as shown by the restoration of the ^{1}H−^{15}N HSQC spectrum of [U-^{15}N]HGD to its native profile as MAC is dialyzed out. The ^{1}H−^{15}N HSQC spectrum also reveals the residues in HGD whose structures are affected upon MAC binding. These residues are spread throughout HGD and are mostly surface-exposed (see Table S1 and Figure 3).

When MAC forms a stable (i.e., irreversible) complex with [U-^{15}N]HGD at higher temperatures where HGD unfolds, some residues show minor CSPs in the ^{1}H−^{15}N HSQC spectrum of [U-^{15}N]HGD and new peaks are observed, while other residues show significant line broadening. This complex did not dissociate upon dialysis and allowed us to specifically define a number of residues in HGD that are affected upon the stable binding of MAC. From these residues, we have selected six as a minimal set that we propose are directly related to MAC binding (see Results for this selection procedure). The involvement of the remaining residues may be a result of local structural changes caused by the binding of MAC as discussed below.

On the basis of our data and the X-ray crystal structure of HGD, we present a structural model of MAC in a complex with HGD. The six residues that we have implicated, namely, Phe 56, Val 132, Val 164, Gly 165, Ser 166, and Leu 167, form a locus spanning the domain interface and a part of the edge

DOI: 10.1021/bi5014479
Biochemistry 2015, 54, 505−515

strand in the C-terminal domain. The length of this locus (measuring the distance between C_α residues) is ~24 Å, roughly the length of the MAC hairpin (see Figure S2A,B). Thus, one can postulate the binding of one strand of MAC with the residues identified in HGD. This would entail the interaction of a strand in MAC with the edge strand (containing residues 164−167) of HGD. The promiscuity of the edge strands of β-sheets in protein−protein interaction and aggregation has been well-documented.[49] Binding of MAC to this edge strand could prevent the aggregation of heat-destabilized HGD.

A computational study[54] of the urea unfolding of HGD has also implicated residues in the domain interface and the C-terminal end. However, this work indicates large structural perturbations in residues 132−164, culminating in domain-swapped polymers. In another study, Zanni and co-workers[55] have shown the involvement of residues 80−163, in the acid denaturation of HGD, using two-dimensional infrared spectroscopy and mass spectrometry. While both these studies implicate residues in the C-terminal end in the unfolding and subsequent aggregation of HGD, the precise locus of residues involved in the process is different from what we find during the heat denaturation of HGD shown here.

We summarize our finding in the model presented in Figure 9 where a surface map of the HGD crystal structure is shown.

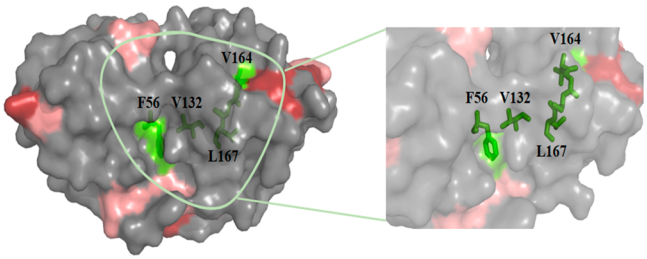

Figure 9. Structural model for HGD−MAC interaction. Surface representation of the crystal structure of HGD (Protein Data Bank entry 1hk0) showing the residues affected by the binding of MAC. Residues affected by reversible binding are shown as red and pink patches (red, stronger binding, lower K_d), (pink, weaker binding, higher K_d). Residues shown as green sticks (F56, V132, and V164−L167), largely in the interior of the protein, are those that are likely to bind irreversibly to MAC when it forms a chaperone−substrate complex with HGD. The molecular surface was rendered semi-transparent to make the buried residues visible. Note that Phe 56 and Val 164 form the two ends of the proposed binding locus.

The red and pink patches on the surface represent residues to which a reversible binding of MAC is observed at ambient temperatures: the red patches show residues with stronger binding (i.e., lower K_d values) and pink patches those with weaker binding (i.e., higher K_d values). The green stick model includes residues of HGD that we propose to be the irreversible binding site for MAC for its chaperone action. They can be seen as an almost contiguous chain running from Phe 56 in the domain interface to Val 132, along with the four residues of a β-strand, namely, Val 164−Leu 167. We calculate the distance between the C_α atoms of the contiguous residues to be around ~24 Å (Table S6). As shown in Figure S2A, all the molecular models of MAC show hairpin-type structures of approximately the same length. Thus, we propose that MAC is likely to bind this locus, primarily in the C-terminal domain through the domain interface in the initial stages of the unfolding of HGD. This could prevent the C-terminal end from collapsing as the target protein unfolds and preserve the domain interface. From their molecular dynamics studies of the urea unfolding of HGD, Das et al.[54] have proposed somewhat similar initial events in the urea unfolding of HGD. Nevertheless, as HGD unfolds, its structure undergoes some expansion, and depending on how the remaining regions of MAC interact with the protein surface, other residues on HGD could also be affected. This in turn would lead to a restructuring of the surface-bound water network. Thus, our current working model of the HGD−MAC complex is that besides the six residues listed here as the ones constituting the binding site for MAC during the initial stages of the unfolding of HGD, other residues show CSPs due to local structural changes as the polypeptide chain of HGD accommodates MAC. Besides Asp 97, which is known to be involved in a charge and water network[46] in HGD, the two terminal residues of the locus implicated in the direct binding of MAC (i.e., Phe 56 and Val 164) also form hydrogen bonds with the hydration layer. The amide groups of Phe 56 form hydrogen bonds with waters 129 and 132, and Val 164 forms hydrogen bonds with water 218 in the crystal structure. Thus, according to this model, the binding of MAC perturbs the hydration layer of HGD and prevents the edge β-strand in the C-terminal end from aggregation. Our data thus show that besides the six residues in HGD implicated directly in binding to MAC, other residues are possibly involved in local structural adjustments of the polypeptide chain of HGD in accommodating MAC. Furthermore, these structural changes may be mediated by the reconfiguration of the water layer surrounding HGD.

The spectroscopic data presented in this report deal with the structures only at equilibrium and do not address the issue of the kinetic aspects of unfolding and precipitation of HGD or the binding of MAC. However, it is conceivable that once the core structure of an HGD domain and the domain interface are disrupted and the hydrophobic residues become solvent-accessible, rapid aggregation would set in. Therefore, we suggest that the reversible low-affinity binding of MAC to the surface of HGD must facilitate the rapid diffusion of MAC to these exposed sites. Such rapid diffusion that results from reducing the dimensionality of the interaction has been observed in various contexts by others and discussed in detail.[56]

In conclusion, we have provided, for the first time, a structural model for the chaperone function of MAC toward HGD. The model highlights the properties of MAC that allow it to function as a molecular chaperone similar to those of the parent α-crystallin. Such observations regarding the "functional mimics" of intact proteins are not entirely unusual. Hochberg et al.[57] have recently shown that a "minimal, chaperone-active unit" of αB-crystallin, which is approximately half the protein, and termed the "core domain", is sufficient to inhibit amyloid fibril formation. Because α-crystallins are now known to chaperone a diverse array of target proteins, MAC and other similar peptides might also be effective in chaperoning proteins other than those already studied.[34,58] Given the importance of the chaperone action of the sHSPs, it would be desirable to engineer more efficient and versatile peptides such as MAC. The work of Nahomi et al.[20] already suggests that an acetylated Lys at the N-terminal end of MAC instead of Asp leads to enhanced chaperone activity of MAC. Our work suggests that modifications of the main turn in the hairpin structure of the peptide, modulating the length of the β-strands in the hairpin, and introducing residues to enhance the reversible binding of

DOI: 10.1021/bi5014479
Biochemistry 2015, 54, 505−515

MAC to the surface of the target are some of the structural manipulations that might affect the chaperone activity of MAC-like peptides and eventually help optimize their function for translational studies.

■ ASSOCIATED CONTENT

Supporting Information

Thermal unfolding of MAC in the far-UV CD region (Figure S1A), best-fit curve through the data from Figure S1A (Figure S1B), structural models of MAC showing a hairpin loop with β-strands (Figure S2A), residues corresponding to MAC in the crystal structure of bovine αA-crystallin (Figure S2B), secondary structure prediction for MAC (Figure S2C), CSPs in the HSQC spectrum of HGD showing irreversible binding of MAC (Figure S3), residues in HGD that show CSPs upon reversible MAC binding (Table S1), residues in HGD that show CSPs upon irreversible MAC binding (Table S2), residues in HGD implicated in irreversible MAC binding with solvent accessibilities (Table S3), potential H-bonds between bound water and selected residues in HGD (Table S4), potential H-bonds between Ser 123 and neighboring residues in HGD (Table S5), and C_α distances computed from the HGD crystal structure (Table S6). This material is available free of charge via the Internet at http://pubs.acs.org.

■ AUTHOR INFORMATION

Corresponding Author

*Department of Chemistry, Life Sciences 2076, University at Albany, State University of New York, 1400 Washington Ave., Albany, NY 12222. E-mail: jpande@albany.edu. Telephone: (518) 591-8842.

Present Address

†P.R.B.: Department of Integrative Structural and Computational Biology, The Scripps Research Institute, La Jolla, CA 92037. E-mail: banerjea@scripps.edu.

Funding

This work was supported by National Institutes of Health Grants GM085006 to A.S. and EY010535 to J.P.

Notes

A preliminary account of a part of this work was presented at the annual meeting of the Association for Research in Vision and Ophthalmology, in Fort Lauderdale, FL, in 2011.

The authors declare no competing financial interest.

■ ABBREVIATIONS

MAC, mini-α-crystallin, a 19-residue peptide of α-crystallin; HGD, human γD-crystallin; sHSPs, small heat-shock proteins; ACD, α-crystallin domain; NMR, nuclear magnetic resonance; CSP, chemical shift perturbation; HSQC, heteronuclear single-quantum coherence; CD, circular dichroism; GdnHCl, guanidinium hydrochloride; TFA, trifluoroacetic acid; UV, ultraviolet.

■ REFERENCES

(1) Slingsby, C., Wistow, G. J., and Clark, A. R. (2013) Evolution of crystallins for a role in the vertebrate eye lens. *Protein Sci. 22*, 367−380.

(2) Berman, E. R. (1991) *Biochemistry of the eye*, Plenum Press, New York.

(3) Slingsby, C., and Clark, A. R. (2013) Flexible nanoassembly for sequestering non-native proteins. *Structure 21*, 193−194.

(4) Basha, E., Lee, G. J., Breci, L. A., Hausrath, A. C., Buan, N. R., Giese, K. C., and Vierling, E. (2004) The identity of proteins associated with a small heat shock protein during heat stress in vivo indicates that these chaperones protect a wide range of cellular functions. *J. Biol. Chem. 279*, 7566−7575.

(5) Eyles, S. J., and Gierasch, L. M. (2010) Nature's molecular sponges: Small heat shock proteins grow into their chaperone roles. *Proc. Natl. Acad. Sci. U.S.A. 107*, 2727−2728.

(6) Jaya, N., Garcia, V., and Vierling, E. (2009) Substrate binding site flexibility of the small heat shock protein molecular chaperones. *Proc. Natl. Acad. Sci. U.S.A. 106*, 15604−15609.

(7) Stengel, F., Baldwin, A. J., Bush, M. F., Hilton, G. R., Lioe, H., Basha, E., Jaya, N., Vierling, E., and Benesch, J. L. (2012) Dissecting heterogeneous molecular chaperone complexes using a mass spectrum deconvolution approach. *Chem. Biol. 19*, 599−607.

(8) Horwitz, J. (1992) α-Crystallin can function as a molecular chaperone. *Proc. Natl. Acad. Sci. U.S.A. 89*, 10449−10453.

(9) Rao, P. V., Horwitz, J., and Zigler, J. S., Jr. (1993) α-Crystallin, a molecular chaperone, forms a stable complex with carbonic anhydrase upon heat denaturation. *Biochem. Biophys. Res. Commun. 190*, 786−793.

(10) Raman, B., Ramakrishna, T., and Rao, C. M. (1997) Effect of the chaperone-like α-crystallin on the refolding of lysozyme and ribonuclease A. *FEBS Lett. 416*, 369−372.

(11) Raman, B., Ramakrishna, T., and Rao, C. M. (1995) Rapid refolding studies on the chaperone-like α-crystallin. Effect of α-crystallin on refolding of β- and γ-crystallins. *J. Biol. Chem. 270*, 19888−19892.

(12) Laganowsky, A., Benesch, J. L., Landau, M., Ding, L., Sawaya, M. R., Cascio, D., Huang, Q., Robinson, C. V., Horwitz, J., and Eisenberg, D. (2010) Crystal structures of truncated αA and αB crystallins reveal structural mechanisms of polydispersity important for eye lens function. *Protein Sci. 19*, 1031−1043.

(13) Basha, E., Friedrich, K. L., and Vierling, E. (2006) The N-terminal arm of small heat shock proteins is important for both chaperone activity and substrate specificity. *J. Biol. Chem. 281*, 39943−39952.

(14) Ghosh, J. G., Shenoy, A. K., Jr., and Clark, J. I. (2006) N- and C-Terminal motifs in human αB crystallin play an important role in the recognition, selection, and solubilization of substrates. *Biochemistry 45*, 13847−13854.

(15) Treweek, T. M., Rekas, A., Walker, M. J., and Carver, J. A. (2010) A quantitative NMR spectroscopic examination of the flexibility of the C-terminal extensions of the molecular chaperones, αA- and αB-crystallin. *Exp. Eye Res. 91*, 691−699.

(16) Delbecq, S. P., Jehle, S., and Klevit, R. (2012) Binding determinants of the small heat shock protein, αB-crystallin: Recognition of the 'IxI' motif. *EMBO J. 31*, 4587−4594.

(17) Bhattacharyya, J., and Sharma, K. K. (2001) Conformational specificity of mini-αA-crystallin as a molecular chaperone. *J. Pept. Res. 57*, 428−434.

(18) Sharma, K. K., Kumar, R. S., Kumar, G. S., and Quinn, P. T. (2000) Synthesis and characterization of a peptide identified as a functional element in αA-crystallin. *J. Biol. Chem. 275*, 3767−3771.

(19) Tanaka, N., Tanaka, R., Tokuhara, M., Kunugi, S., Lee, Y. F., and Hamada, D. (2008) Amyloid fibril formation and chaperone-like activity of peptides from αA-crystallin. *Biochemistry 47*, 2961−2967.

(20) Nahomi, R. B., Wang, B., Raghavan, C. T., Voss, O., Doseff, A. I., Santhoshkumar, P., and Nagaraj, R. H. (2013) Chaperone peptides of α-crystallin inhibit epithelial cell apoptosis, protein insolubilization, and opacification in experimental cataracts. *J. Biol. Chem. 288*, 13022−13035.

(21) Sreekumar, P. G., Chothe, P., Sharma, K. K., Baid, R., Kompella, U., Spee, C., Kannan, N., Manh, C., Ryan, S. J., Ganapathy, V., Kannan, R., and Hinton, D. R. (2013) Antiapoptotic properties of α-crystallin-derived peptide chaperones and characterization of their uptake transporters in human RPE cells. *Invest. Ophthalmol. Visual Sci. 54*, 2787−2798.

(22) Quach, Q. L., Metz, L. M., Thomas, J. C., Rothbard, J. B., Steinman, L., and Ousman, S. S. (2013) CRYAB modulates the activation of CD4+ T cells from relapsing-remitting multiple sclerosis patients. *Mult. Scler. 19*, 1867−1877.

DOI: 10.1021/bi5014479
Biochemistry 2015, 54, 505−515

(23) Kurnellas, M. P., Adams, C. M., Sobel, R. A., Steinman, L., and Rothbard, J. B. (2013) Amyloid fibrils composed of hexameric peptides attenuate neuroinflammation. *Sci. Transl. Med. 5*, 179ra142.
(24) Stern, J. H. (2013) Mini-Chaperones for Early AMD. *Invest. Ophthalmol. Visual Sci. 54*, 2799.
(25) Andley, U. P., Malone, J. P., and Townsend, R. R. (2014) In Vivo Substrates of the Lens Molecular Chaperones αA-crystallin and αB-crystallin. *PLoS One 9*, e95507.
(26) Pande, A., Pande, J., Asherie, N., Lomakin, A., Ogun, O., King, J. A., Lubsen, N. H., Walton, D., and Benedek, G. B. (2000) Molecular basis of a progressive juvenile-onset hereditary cataract. *Proc. Natl. Acad. Sci. U.S.A. 97*, 1993−1998.
(27) Pande, A., Zhang, J., Banerjee, P. R., Puttamadappa, S. S., Shekhtman, A., and Pande, J. (2009) NMR study of the cataract-linked P23T mutant of human γD-crystallin shows minor changes in hydrophobic patches that reflect its retrograde solubility. *Biochem. Biophys. Res. Commun. 382*, 196−199.
(28) Banerjee, P. R., Pande, A., Patrosz, J., Thurston, G. M., and Pande, J. (2011) Cataract-associated mutant E107A of human γD-crystallin shows increased attraction to α-crystallin and enhanced light scattering. *Proc. Natl. Acad. Sci. U.S.A. 108*, 574−579.
(29) Fasman, G. D. (1976) *Handbook of biochemistry and molecular biology*, 3rd ed., CRC Press, Cleveland.
(30) Acosta-Sampson, L., and King, J. (2010) Partially folded aggregation intermediates of human γD-, γC-, and γS-crystallin are recognized and bound by human αB-crystallin chaperone. *J. Mol. Biol. 401*, 134−152.
(31) Cavanagh, J. (2007) *Protein NMR spectroscopy: Principles and practice*, 2nd ed., Academic Press, Amsterdam.
(32) Piotto, M., Saudek, V., and Sklenar, V. (1992) Gradient-tailored excitation for single-quantum NMR spectroscopy of aqueous solutions. *J. Biomol. NMR 2*, 661−665.
(33) Masse, J. E., and Keller, R. (2005) AutoLink: Automated sequential resonance assignment of biopolymers from NMR data by relative-hypothesis-prioritization-based simulated logic. *J. Magn. Reson. 174*, 133−151.
(34) Raju, M., Santhoshkumar, P., and Sharma, K. K. (2012) αA-Crystallin-derived mini-chaperone modulates stability and function of cataract causing αAG98R-crystallin. *PLoS One 7*, e44077.
(35) Santhoshkumar, P., and Sharma, K. K. (2004) Inhibition of amyloid fibrillogenesis and toxicity by a peptide chaperone. *Mol. Cell. Biochem. 267*, 147−155.
(36) Sreelakshmi, Y., and Sharma, K. K. (2001) Interaction of α-lactalbumin with mini-αA-crystallin. *J. Protein Chem. 20*, 123−130.
(37) Kumar, R. S., and Sharma, K. K. (2000) Chaperone-like activity of a synthetic peptide toward oxidized γ-crystallin. *J. Pept. Res. 56*, 157−164.
(38) Raju, M., Santhoshkumar, P., Xie, L., and Sharma, K. K. (2014) Addition of αA-crystallin sequence 164−173 to a mini-chaperone DFVIFLDVKHFSPEDLT alters the conformation but not the chaperone-like activity. *Biochemistry 53*, 2615−2623.
(39) Kurnellas, M. P., Brownell, S. E., Su, L., Malkovskiy, A. V., Rajadas, J., Dolganov, G., Chopra, S., Schoolnik, G. K., Sobel, R. A., Webster, J., Ousman, S. S., Becker, R. A., Steinman, L., and Rothbard, J. B. (2012) Chaperone activity of small heat shock proteins underlies therapeutic efficacy in experimental autoimmune encephalomyelitis. *J. Biol. Chem. 287*, 36423−36434.
(40) Barrow, C. J., Yasuda, A., Kenny, P. T., and Zagorski, M. G. (1992) Solution conformations and aggregational properties of synthetic amyloid β-peptides of Alzheimer's disease. Analysis of circular dichroism spectra. *J. Mol. Biol. 225*, 1075−1093.
(41) Yang, J. J., Pikeathly, M., and Radford, S. E. (1994) Far-UV circular dichroism reveals a conformational switch in a peptide fragment from the β-sheet of hen lysozyme. *Biochemistry 33*, 7345−7353.
(42) Maupetit, J., Derreumaux, P., and Tuffery, P. (2009) PEP-FOLD: An online resource for de novo peptide structure prediction. *Nucleic Acids Res. 37*, W498−W503.
(43) Neron, B., Menager, H., Maufrais, C., Joly, N., Maupetit, J., Letort, S., Carrere, S., Tuffery, P., and Letondal, C. (2009) Mobyle: A new full web bioinformatics framework. *Bioinformatics 25*, 3005−3011.
(44) Baxter, N. J., and Williamson, M. P. (1997) Temperature dependence of ^{1}H chemical shifts in proteins. *J. Biomol. NMR 9*, 359−369.
(45) Ghosh, K. S., Pande, A., and Pande, J. (2011) Binding of γ-crystallin substrate prevents the binding of copper and zinc ions to the molecular chaperone α-crystallin. *Biochemistry 50*, 3279−3281.
(46) Basak, A., Bateman, O., Slingsby, C., Pande, A., Asherie, N., Ogun, O., Benedek, G. B., and Pande, J. (2003) High-resolution X-ray crystal structures of human γD crystallin (1.25 Å) and the R58H mutant (1.15 Å) associated with aculeiform cataract. *J. Mol. Biol. 328*, 1137−1147.
(47) Kastritis, P. L., van Dijk, A. D., and Bonvin, A. M. (2012) Explicit treatment of water molecules in data-driven protein-protein docking: The solvated HADDOCKing approach. *Methods Mol. Biol. 819*, 355−374.
(48) Soda, K., Shimbo, Y., Seki, Y., and Taiji, M. (2011) Structural characteristics of hydration sites in lysozyme. *Biophys. Chem. 156*, 31−42.
(49) Richardson, J. S., and Richardson, D. C. (2002) Natural β-sheet proteins use negative design to avoid edge-to-edge aggregation. *Proc. Natl. Acad. Sci. U.S.A. 99*, 2754−2759.
(50) Williamson, M. P. (2013) Using chemical shift perturbation to characterise ligand binding. *Prog. Nucl. Magn. Reson. Spectrosc. 73*, 1−16.
(51) Stark, J., and Powers, R. (2008) Rapid protein-ligand costructures using chemical shift perturbations. *J. Am. Chem. Soc. 130*, 535−545.
(52) Breiten, B., Lockett, M. R., Sherman, W., Fujita, S., Al-Sayah, M., Lange, H., Bowers, C. M., Heroux, A., Krilov, G., and Whitesides, G. M. (2013) Water networks contribute to enthalpy/entropy compensation in protein-ligand binding. *J. Am. Chem. Soc. 135*, 15579−15584.
(53) Bova, M. P., Ding, L. L., Horwitz, J., and Fung, B. K. (1997) Subunit exchange of αA-crystallin. *J. Biol. Chem. 272*, 29511−29517.
(54) Das, P., King, J. A., and Zhou, R. (2011) Aggregation of γ-crystallins associated with human cataracts via domain swapping at the C-terminal β-strands. *Proc. Natl. Acad. Sci. U.S.A. 108*, 10514−10519.
(55) Moran, S. D., Decatur, S. M., and Zanni, M. T. (2012) Structural and sequence analysis of the human γD-crystallin amyloid fibril core using 2D IR spectroscopy, segmental ^{13}C labeling, and mass spectrometry. *J. Am. Chem. Soc. 134*, 18410−18416.
(56) Berg, O. G., and von Hippel, P. H. (1985) Diffusion-controlled macromolecular interactions. *Annu. Rev. Biophys. Biophys. Chem. 14*, 131−160.
(57) Hochberg, G. K., Ecroyd, H., Liu, C., Cox, D., Cascio, D., Sawaya, M. R., Collier, M. P., Stroud, J., Carver, J. A., Baldwin, A. J., Robinson, C. V., Eisenberg, D. S., Benesch, J. L., and Laganowsky, A. (2014) The structured core domain of αB-crystallin can prevent amyloid fibrillation and associated toxicity. *Proc. Natl. Acad. Sci. U.S.A. 111*, E1562−E1570.
(58) Rothbard, J. B., Kurnellas, M. P., Brownell, S., Adams, C. M., Su, L., Axtell, R. C., Chen, R., Fathman, C. G., Robinson, W. H., and Steinman, L. (2012) Therapeutic effects of systemic administration of chaperone αB-crystallin associated with binding proinflammatory plasma proteins. *J. Biol. Chem. 287*, 9708−9721.

DOI: 10.1021/bi5014479
Biochemistry 2015, 54, 505−515